METEC & 6TH ESTAD 2023

Solidification microstructure of a continuously cast HSLA steel slab with U-shape centerline segregation

Gilberson M Storck de Melo*, Afrânio M Costa*, André A Nascimento*, Alisson P Oliveira**, Antonio A Gorni**, Gabrielly L Oliveira[X], Jose M Ibabe[+].

* Gerdau - Ouro Branco steelworks: Rod. MG-443, Km 7 s/n - Fazenda do Cadete, Ouro Branco, MG, ZIP: 36490-972, Brazil;
** CBMM: Avenida Brigadeiro Faria Lima, 4285, 9th floor, São Paulo, SP, ZIP: 04538-133, Brazil;
[X] Universidade Federal de Minas Gerais: Avenida Presidente Antônio Carlos, 6627, Pampulha, Belo Horizonte, MG, ZIP: 31270-901, Brazil;
[+] CEIT: Paseo de Manuel Lardizabal, 15 Donostia - San Sebastián, ZIP: 20018, Spain.

Summary

Macro and microsegregation play an important role in understanding the solidification behavior of continuously cast steels. Both affects directly critical applications, which requires a higher degree of homogeneity since as the cast stage. This study applied macro and micro approaches to perform a comprehensive characterization of the solidification of a slab with U-shape centerline segregation. In the macro-approach, thickness and width-wise chemical analysis was performed using OES on whole centerline. C, P, S, Ti and Nb contents in centerline was almost 3 times higher than base chemistry. The micro-approach in this study considered metallography of ferritic matrix and its constituents, as well as SDAS (Secondary Dendrite Arm Spacing). Calculated figures of SDAS presented very good correspondence with measured ones. *Liquidus* and *solidus* position, as well as mushy zone was calculated using CON1D model. Based on these results, which measured values were in good agreement with calculated ones, it is possible to estimate the internal quality of slabs in a higher degree of confidence.

Key words: steel, continuous casting, macrosegregation, centerline segregation, solidification microstructure.

1 Introduction

As has already been widely reported in the technical literature, the segregation that occurs in the continuous casting of steels can be on a microscopic scale, arising from the last liquid that solidifies between the dendrites, and on a scale like that of the strand, in its core, which are respectively designated as being micro and macro-segregation. It is virtually impossible to eliminate the distribution of alloy element concentrations established by the segregation that occurs during solidification, which ends up being inherited even by successively hot-rolled, cold-rolled and annealed flat products [1]. The most common manifestation of this pattern is the presence of microstructure banding, that is, alternating longitudinal bands of ferrite and pearlite. The costly normalizing heat-treatment can remove pearlite banding, but it is non-capable to full remove the micro-segregation pattern in the alloy [2]. The lack of segregation control can strongly impact the performance of the final steel product in the most diverse ways [3].

The continuous evolution of the quality of steel products, together with the pressure to reduce their costs, motivated the execution of numerous studies aimed at understanding and modeling the metallurgical phenomena associated with segregation. One of the most remarkable works in this sense was developed by [4], based on the Clyne-Kurz model [5] and which is part of the global model for one-dimensional heat transfer and solidification during continuous slab casting, CON1D [6], which has been continuously improved over the past decades by the Continuous Casting Consortium. Another alternative that has been widely used recently is the simulation of solidification and the consequent segregation using computational thermodynamics packages, such as ThermoCalc and FactSage. Artificial Intelligence is also being used in this context [7].

A previous study, carried out cooperatively between Gerdau Ouro Branco and CBMM, characterized the influence of micro-segregation on the formation of the microstructure and, particularly, the size distribution of microalloy precipitates in the interdendritic region of the plates [8]. This last work, constitutes the starting point for more specific studies on continuous casting of slabs, now also involving the Continuous Casting Consortium (CCC). In the present work, the “U” pattern of centerline segregation that occurs in the continuous casting of slabs at this plant was characterized in detail.

2 Testing Methods

2.1 Macro analysis

An industrial experiment was performed on a continuously cast HSLA Nb-Ti microalloyed grade. A sample was taken from tundish after homogenization. **Table 1** shows details of chemical composition that, hereafter, will be nominated as “base chemistry”. Among the elements in steel chemical composition, this present work selects the six more relevant elements for segregation. This pick considers the partition and diffusion coefficients in delta ferrite and austenite [9].

Table 1. Base chemistry of test heat – mass content in % wt.

C	Mn	Nb	Ti	P	S
0.15	1.35	0.026	0.015	0.021	0.005

Test heat produced 250mm x 2100mm slab. During the casting, a sample of 80mm long was taken. After air cooling, the slab sample was cut into 07 pieces, according to **figure 1a,** and then ground and etched with HCl, to reveal slab macrostructure and its centerline segregation. After that, smaller pieces were cut in thickness-wide and width-wide strategy for five macro-etch samples as stated in **figure 1a**. These pieces were ground again and sent to an Optical Emission Spectrometer (OES) to analyze the chemical composition at the points defined in **figure 1b and 1c**. The main goal was to determine the differences between the base chemistry shown in **table 1** and local chemical composition.

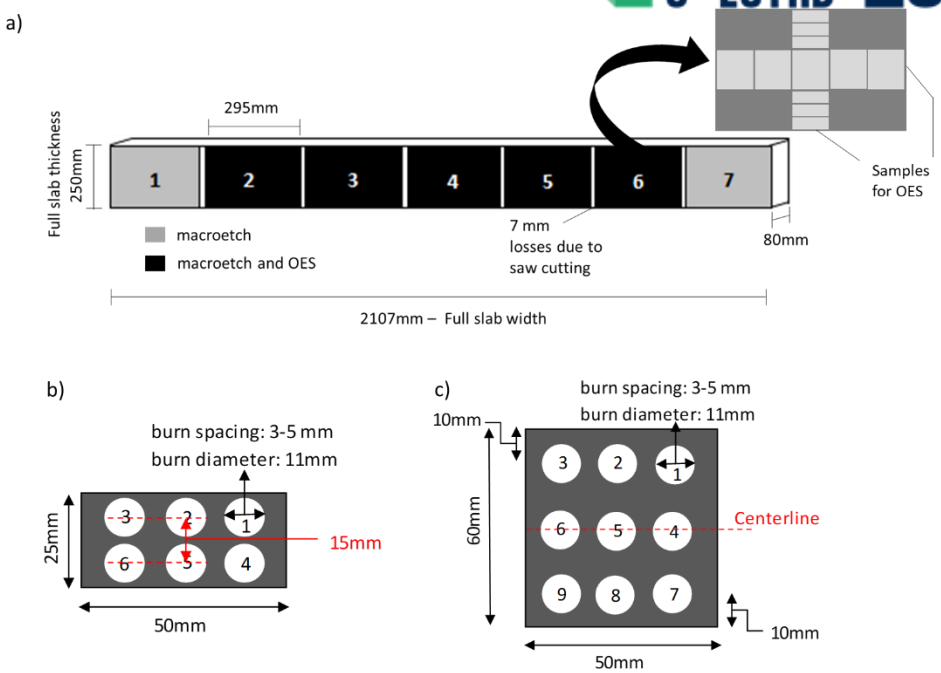

Figure 1. (a) Samples for macro-etch taken from slab width, detailing smaller samples for OES. (b) Thickness-wide sample for OES. (c) Width-wide sample for OES.

Furthermore, from chemical analysis stated in **figure 1**, it was possible to identify fields of higher concentration throughout slab width and thickness. In case of width, two well defined fields of higher concentration define a U-shape centerline segregation. Both segregation fields are almost mirrored considering the center slab width.

2.2 Microanalysis

After identifying the fields of higher concentration that defines U-shape, among the samples 2 – 6 (**figure 1**), it was selected two samples: one that has fields with higher concentration and another one without pronounced segregation. Metallography for determination of steel matrix features and dendritic microstructure was carried out on samples at 37.5mm below slab top surface (inner radius) and centerline to compare the differences between last portion to solidify (centerline) and an intermediate point. For that, two different etchants were used: Nital 2%, for the first determination and Picral 2% for second one.

2.2.1 SDAS measurements

During the solidification process, solid dendrites and interdendritic liquid coexist at mushy zone. Segregation pattern is largely influenced by microstructural length scales of dendrites, especially secondary dendrite arm spacing (SDAS) [10]. This present work measured and calculated the SDAS. The first one was done by intercept method using optical micrographs taken by metallurgical microscope instrumented with CCD camera and proper image analysis software. SDAS calculation is described in next section.

3 Calculations

3.1 Secondary Dendrite Arm Spacing (SDAS)

Several empirical relationships have been reported elsewhere [11], and almost all of them made a relationship with solidification time or cooling rate. Some of them also reported influence of carbon content as an argument of their equations [4, 11, 12]. Based on that, SDAS measurements can provide important information to estimate solidification process. This paper uses the empirical relationship reported by Won and Thomas [4] which are coupled in CON1D model [4, 6].

3.2 Continuous casting solidification process

This present work will apply the well know and widely reported continuous casting solidification model CON1D. Process parameters of test heat and geometrical parameters of Gerdau Ouro Branco steelworks slab caster machine was fed into the model, to have outputs like *solidus* and *liquidus* position and length of mushy zone, cooling rates and local solidification time. The last two support SDAS calculations. **Table 2** displays most relevant inputs for this calculation.

Table 2. Some relevant casting data obtained by test heat and used as input data in CON1D.

Input data	value	Input data	value
Slab section [mm]	250 x 2100	Mold geometry	straight
Super heat [°C]	25°C	Mold length [mm]	800
Casting speed [m/min]	0.90	Roll radius [mm]	75, 115, 150
Metallurgical length [m]	36.9	Spray angle [deg]	95, 105, 110

Remarks: mold length considers from meniscus to mold end

4 Results and discussion

4.1 Macro analysis

Figure 2 shows a concentration map for C, Mn, Nb, Ti, S and P for samples 2 to 6. Each little square represents an individual analysis, as previously seen in **figure 1**. Dark areas mean higher concentration. Virtually, there is no significant variation from slab surface up to 112mm below both surfaces (inner and outer radius). This figure also characterizes the U-shape segregation in slab, where portions with severe segregation (sample 3 and region between sample 5 and 6) probably comes from the prominent parts of solidification front. The center of slab (sample 4) would represent the later portion of solidification front. With exception to Mn, the concentration of other elements can reach almost 2 to 3 times higher than base chemistry. Although a concentration increase can be seen in centerline of sample 4 (center of width), it's just around 30% higher than base chemistry. A recent work [13] reported that increase in concentration of C, P and S in centerline segregation peak is almost the double. Another author [14] reported that an increase of 3.3 times in C concentration was found in a calculation considering solid fraction 0.99 for wide and heavy peritectic slabs with 0.13% wt. as base concentration. The macro segregation pattern, observed in this present work, possibly, can be credited to an unbalanced secondary cooling on slab wide surface. Additionally, after soft reduction, a possible trapping of enriched final liquid present in protuberant parts of solidification front can be related to portions where severe centerline segregation was found.

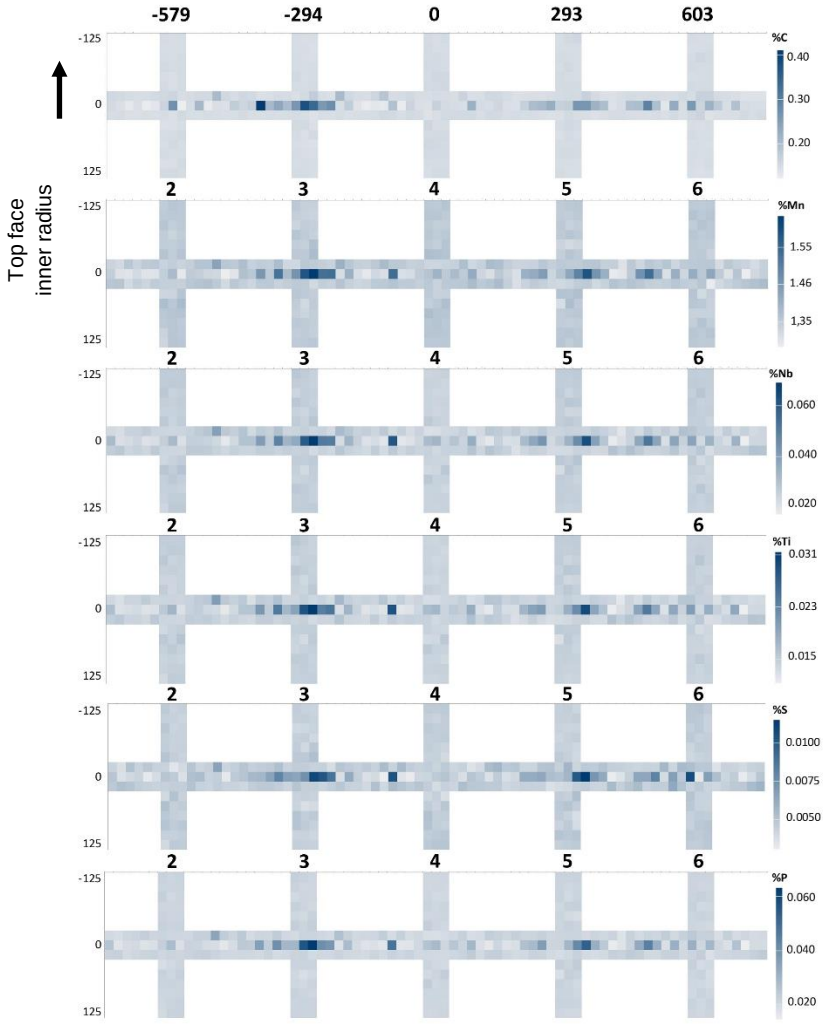

Figure 2. Concentration map for C, Mn, Nb, Ti, S and P for samples 2 to 6.

4.2 Micro analysis

Figure 3 and **Figure 4** show metallography of steel matrix features and dendritic microstructure respectively for sample 3, containing severe segregation and sample 4 with no relevant segregation. As it can be seen, through **figure 3**, SDAS and steel matrix at centerline segregation is very different from intermediate portion (37.5mm). Pearlite colonies presented in **figure 3c** suggests a high carbon grade while steel matrix and constituents observed in **figure 3a** match with peritectic-medium carbon grade of base chemistry. Solidification microstructure given by **figures 3b** and **3d** follow the same pattern. The second one, which refers to centerline segregation, presents thinner secondary dendrite arms when compared to intermediary portion. This fact influences directly SDAS measures, which is directly linked to higher carbon content and solute enrichment in centerline.

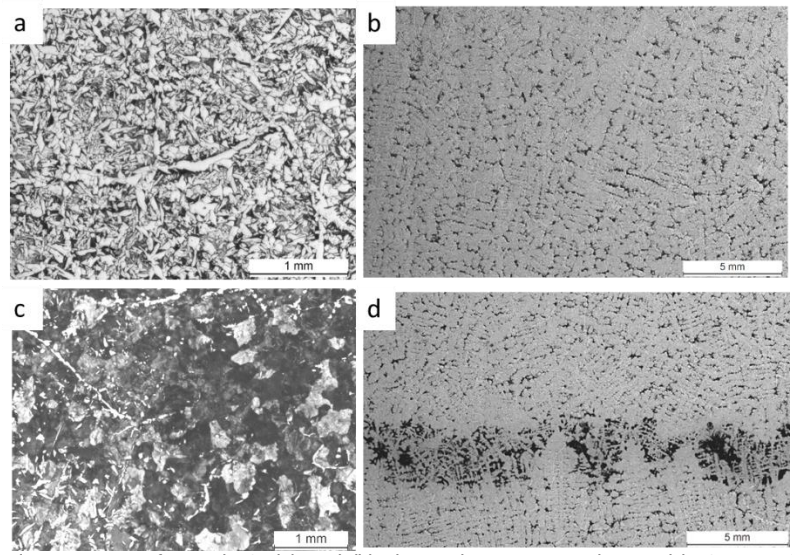

Figure 3. Microstructure of sample 3. (a) and (b) show microstructure observed in 37.5mm below top surface – inner radius. (c) and (d) microstructure observed in centerline segregation

Although a difference between intermediate position (37.5mm) and centerline could be observed in **Figure 4**, there is a slight contrast between the two positions. Steel matrix and its constituents in centerline agrees well with an expected level of segregation of a regular HSLA grade with 0.15% C, without any casting issues which could decrease internal quality of slabs.

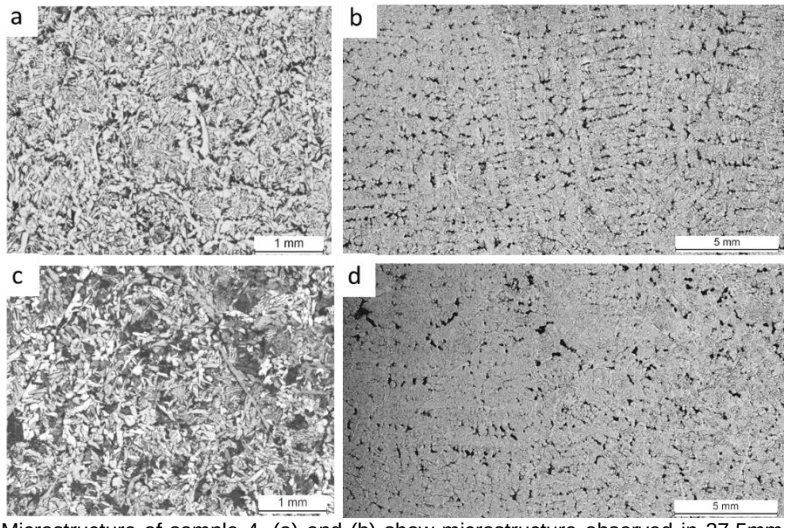

Figure 4. Microstructure of sample 4. (a) and (b) show microstructure observed in 37.5mm below top surface – inner radius. (c) and (d) microstructure observed in centerline segregation

4.3 SDAS measurement and calculations

SDAS was estimated based on actual values for water flow in primary and secondary cooling zones. Margin zones were considered to run a calculation for sample 3 and center zones were considered to run a calculation for sample 4. For the cooling practice applied for present steel grade, there is little difference between them. **Figure 5** shows a comparative between measurements and calculation.

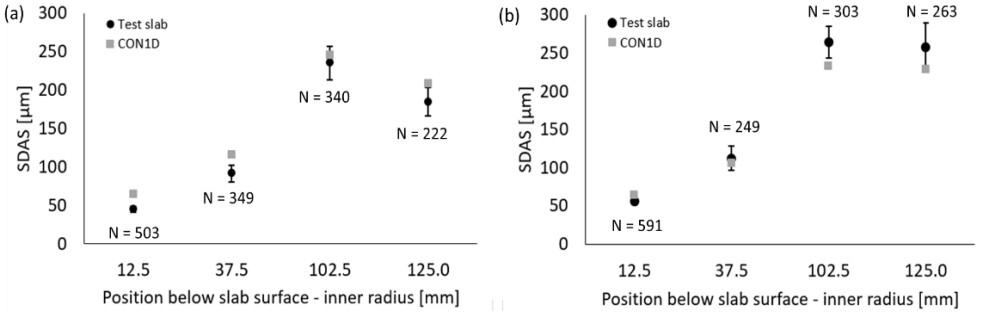

Figure 5. SDAS comparisons between Test slab and CON1D. (a) Sample 3 – severe segregation (b) Sample 4 – light segregation. Upper and Lower bars mean 1 standard deviation of measurements (N) in test slab for each position

CON1D results presented the same behavior as measurements performed in test slab. It was observed few differences in the SDAS calculations between the samples. The most relevant one is a considerable SDAS drop in the last two measurements and calculations observed in sample 3. This fact could be explained by liquid enrichment point of view: *liquidus* and *solidus* temperature decreases and, consequently, solidification time also decreases. As SDAS is proportional to solidification time [4, 6, 11, 12], the observed behavior is expected. The same could be used for sample 4: The last two SDAS (102.5 and 125.0mm) was almost the same for measurements and calculations: it means that last liquid was not too much different from the 102.5mm position and, consequently, solidification time of two last positions was almost the same.

4.4 Continuous casting solidification process

Figure 6 represents a longitudinal view of strand mushy zone. This figure shows both *liquidus* and *solidus* positions, as well as the length of mushy zone for each case: test slab - data informed by supervisory system of continuous casting machine and CON1D simulation, which used a data set of test slab extracted by caster test server. As it can be seen, a difference of 150mm in *liquidus* position is very small when compared to segments and rolls dimensions. Positions close to 14.5m in CC machine has a roll diameter with 230mm. It suggests that difference between CON1D and caster data is lower than a roll. *Solidus* position, which is more sensible to casting process and its variations, was estimated by CON1D as 730mm earlier than caster data. At 21m inside the caster, the diameter of rolls is a little bit higher: 300mm. It means that the difference between CON1D and caster data are almost 2.5 rolls. Since all segments have 7 rows of rolls, the differences found for both positions are very small and, based on these results, CON1D estimations were very adherent with caster industrial data.

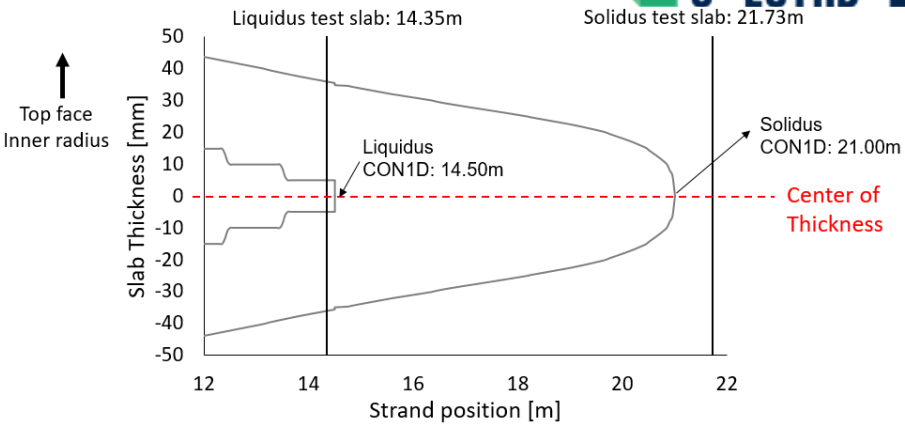

Figure 6. Representation of a longitudinal view of strand mushy zone, with *liquidus* and *solidus* point comparisons between caster data and CON1D estimations.

5 Conclusions

The method of macro and micro segregation assessment presented here has done its homework by establishing a method to identify and measure the intensity of U pattern segregation in a wide slab. CON1D present itself as a good and reliable tool for simulation, once its estimations were very adherent with caster industrial data.

6 References

[1] Preβlinger, H., Mayr, M., Tragl, E., Bernhard, C.: steel res. 77, 107-115 (2006), 2.
[2] Spitizig, W.: Metall. Trans. A, 271-283 (1983), 14.
[3] Lage, M., Costa e Silva, A., Mater. Res., 353-358 (2015), 4(4).
[4] Won, Y., Thomas, B.: Metall. Trans. A, 1755-1767 (2001), 32A.
[5] Clyne, T. W., Kurz, W.: Metall. Trans. A, 965-970 (1981), 12A.
[6] Meng, Y., Thomas, B.: Metall. Trans. B, 685-705 (2003), 34B.
[7] Zhang, P., Minglin, W., Shi, P., Xu, L.: Metals, 1826-1844 (2022), 12.
[8] Escobar, D., Castro, C., Borba, E., Oliveira, A., Camey, K., Taiss, E., Costa e Silva, A., Spangler, M., Metall. Trans. A, 3358-3372 (2018), 49A.
[9] Zhang, D.: Characterization and modelling of segregation in continuously cast steel slab. (University of Birmingham Electronic Thesis Library) https://etheses.bham.ac.uk/id/eprint/6256/1/ZhangD15PhD.pdf Accessed 24 April 2023
[10] Straffelini, G., Lutterotti, L., Tonolli, M., Lestani, M.: ISIJ Int., 1448-1453 (2011), 51(9)
[11] Weisgerber, B., Hecht, M., Harste, H.: steel res. 70, 403-411 (1997), 10.
[12] Pierer, R., Bernhard, C.: J Mater Sci., 6938-6943 (2008), 43.
[13] Quinelato, F., Garção, W., Paradela, K., Sales, R., Baptista, L., Ferreira, A.: Mater. Res., 1-9 (2020), 23(4).
[14] Wang, W., Zhu, M., Cai, Z., Luo, Sem., Ji, C., steel res. 83, 1152-1162 (2012), 12.